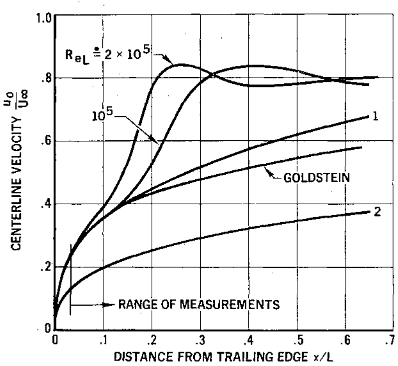

Fig. 1 Experiment of Sato and Kuriki (plate I, Ref. 9) as compared with Goldstein's result,[10] the corresponding similarity solution (case 1, $c = 0$), and the present similarity solution (case 2, $l_1 = l_2 = 0$).

and, 2) the upstream effect on the wall shear by

$$\tau/\tau_{-\infty} = 1 + 0.254\,[|x|(\Omega/\nu)^{1/2}]^{-2/3} - 0.004[|x|(\Omega/\nu)^{1/2}]^{-4/3} + \ldots \quad (11)$$

It is interesting to note that there is apparently a sizable range of $|x|(\Omega/\nu)^{1/2}$ where τ/τ_∞ turns out to be larger than 1. The reason is that the fluid entering the wake is accelerated, and the corresponding "displacement effect" (caused by the "negative displacement thickness" of the wake) increases the upstream velocity and the shear. In order to estimate the region of validity of the similarity solution, the first term in the asymptotic expansion (10), one sees that for

$$[|x|_{\lim}(\Omega/\nu)^{1/2}]^{-2/3} = 0.4 \quad (12)$$

the known consecutive terms in Eq. (11) decrease by at least a factor of 0.1, and the terms in Eq. (10) also decrease reasonably fast. It is also reassuring to note that the form of (12) is compatible with an outer limit of validity criterion based on Imai's proposed theory for flow in the vicinity of a trailing edge.[8]

Now, the validity of the theory presented in this paper, including the effect of the vorticity-induced pressure gradient, supposes x to be less than δ_{Bl} from Eq. (9) but larger than $|x|_{\lim}$ after Eq. (12), i.e.,

$$|x|_{\lim}/L = 7Re_L^{-3/4} < x/L < 5Re_L^{-1/2} \cong \delta_{Bl}/L \quad (13)$$

For

$$Re_L = 10^2,\ 0.48 < x/L < 0.50$$

$$Re_L = 3 \times 10^3,\ 0.018 < x/L < 0.09$$

$$Re_L = 10^5,\ 0.001 < x/L < 0.015$$

It is seen that the Reynolds number must be sufficiently large to provide a separation between the upper and lower limits or validity; on the other hand, it should remain well below the laminar stability limit. In this range of Reynolds numbers, the vorticity-induced pressure gradient should then be observable in a small region near the trailing edge. Whether or not actual measurements are indeed possible depends, of course, on the size of the experimental apparatus relative to the physical extent of the region under consideration.

At this time, the only applicable experimental investigation of the merging of two Blasius boundary layers is that carried out by Sato and Kuriki.[9] Reynolds number range extended from approximately 10^5 to 2×10^5; in this range, the possible existence of the vorticity-induced pressure gradient region can be anticipated. According to Eq. (9), the boundary-layer thickness δ_{Bl}/L varied from 0.015 to 0.01, whereas $|x|_{\lim}/L$ was bracketed by the values 0.001 and 0.0006.

Figure 1 shows the measurements of u_0/U_∞ by Sato and Kuriki,[9] together with theoretical curves after Goldstein,[3,10] and with the inclusion of the vorticity-induced pressure gradient effect (curve 2). The points measured by Sato and Kuriki begin at $x = 10$mm; this gives, with a plate length $L = 3000$ mm, $x/L = 3 \times 10^{-2}$, which lies outside of the discernible pressure gradient effect region for the Reynolds numbers of the test. Indeed, the measurements of Sato and Kuriki follow Goldstein's curve closely, before the effect of instability takes over and leads to major deviations from curve 1.

Although the measurements of Sato and Kuriki do not penetrate into the predicted region of validity for curve 2, Fig. 1 nevertheless illustrates the difficulties of an experiment that is designed to discern between curves 1 and 2 in that region. At the present time, experimental evidence concerning the existence of an induced pressure gradient in merging shear flows must be considered inconclusive.

References

[1] Rott, N. and Hakkinen, R. J., "Similar solutions for merging shear flows," J. Aerospace Sci. **29,** 1134–1135 (1962).

[2] Rott, N. and Hakkinen, R. J., "Numerical solutions for merging shear flows," Douglas Aircraft Co., Inc., Rept. SM-47809 (July 1965).

[3] Goldstein, S., "Concerning some solutions of the boundary layer equations in hydrodynamics," Proc. Cambridge Phil. Soc. **26,** 1–30 (1930).

[4] Li, T. Y., "Effects of free stream viscosity on the behavior of a viscous boundary layer," J. Aeronaut. Sci. **23,** 1128–1129 (1956).

[5] Murray, T. D., "The boundary layer on a flat plate in a stream with uniform shear," J. Fluid Mech. **11,** Pt. 2, 309–316 (1961).

[6] Toomre, A. and Rott, N., "On the pressure induced by the boundary layer on a flat plate in shear flow," J. Fluid Mech. **19,** Pt. 1, 1–10 (1964).

[7] Hakkinen, R. J. and O'Neil, E. J., "Higher approximations for merging of uniform shear flows," Douglas Aircraft Co., Inc., Paper 3050 (to be published).

[8] Imai, I., "On the viscous flow near the trailing edge of a flat plate," *Proceedings of the XIth International Congress of Applied Mechanics* (Springer: Julius Springer-Verlag, Berlin, to be published).

[9] Sato, H. and Kuriki, K., "The mechanism of transition in the wake of a thin flat plate placed parallel to a uniform flow," J. Fluid Mech. **11,** Pt. 3, 321–352 (1961).

[10] Goldstein, S., "On the two-dimensional steady flow of a viscous fluid behind a solid body I," Proc. Roy. Soc. (London) **A142,** 545–560 (1933).

Shock Predictions in Conical Nozzles

D. Migdal* and R. Kosson†
Grumman Aircraft Engineering Corporation, Bethpage, N. Y.

Introduction

PREVIOUS analyses indicate that conventional conical nozzles are not shock free[1,2] and that the initial shock formation occurs near the axis of symmetry.[2] There are several applications where the formation of a shock in this region is of importance. For example, conventional conical nozzles are often used to study nonequilibrium flow,[3,4] and there exists the possibility of obscuring the chemical effects with aerodynamic factors. In the study of flow over bodies placed along the centerline of conical wind-tunnel nozzles, the freestream conditions cannot be properly assessed without a knowledge of the effects of shock formation; and for the same reason, the design of contoured wind-tunnel nozzles

Received March 16, 1965; revision received April 29, 1965.

* Project Leader, Gas Dynamics Group, Thermodynamics and Propulsion Section.

† Group Leader, Advanced Development, Thermodynamics and Propulsion Section.

based on the assumption of an initial source flow will not lead to completely predictable test section conditions.

Despite the practical significance, in the foregoing applications, complete experimental verification of the shock formation is unavailable. It is the purpose of this note to discuss some of the physical phenomena that lead to the shock formation and to provide analytical predictions of the shock strength which can be used as the basis for experimental studies. Experimental studies will be required to determine the extent to which the boundary layer modifies the shock formation.

Discussion

As used here, a conventional conical nozzle includes a cone attached directly to the throat (Fig. 1) or a cone attached to a contour with constant radius of curvature (Fig. 1). The assumptions and method of analysis outlined in Ref. 5 were used here. The irrotational method of characteristics for axisymmetric flow was employed, and numerical solutions were obtained with the IBM 7094. Crossing of the same family of Mach waves denoted the formation of a shock. The pressure rise is treated as an isentropic compression. This assumption yields a higher value of the shock strength (measured in terms of pressure ratio) than the use of oblique shock relations. For the flow deflections and Mach numbers considered in this study, the errors in pressure ratio were found to be less than 2%.

Results

Many conical nozzles were analyzed. In all cases the crossing of Mach waves near the nozzle axis could be traced to the contour junction with the conical section as in Ref. 2. Continued calculations revealed a decay in the reflected shock strength, so that in most cases there was no discernible pressure rise along the contour. It thus appears that if the shock is to be detected experimentally it must be done by examining the interior of the flow, especially in the vicinity of the nozzle axis.

Typical results of the pressure distribution along the axis are shown in Fig. 2. The static pressure is divided by the chamber value, the distance (X) is referred to the throat radius (R^*), various circular arc radii of curvature (R_c) are joined to a 15° wall-angle nozzle, and the ratio of specific heats was taken as 1.4. The results (Fig. 2) indicate that the pressure rise occurs within a very narrow region, and that increasing the throat radius of curvature shifts the axial location of the shock downstream and diminishes the shock strength.

In examining the region where the cone is attached to the contour (or directly to the throat), a discontinuous change in local radius of curvature is observed. This fact, by itself, gives no clue as to the cause of shock formation, since identical results with planar flow indicate shock-free flow. The physical phenomena that lead to shock formation are thus due entirely to axisymmetric effects. In all cases, the calculation results reveal that downstream of the contour junction the streamlines near the wall are inclined at a larger flow angle than the wall itself (Fig. 1c). Thus, a compressive turning is required to satisfy the wall boundary conditions, and this is the beginning of the shock formation.

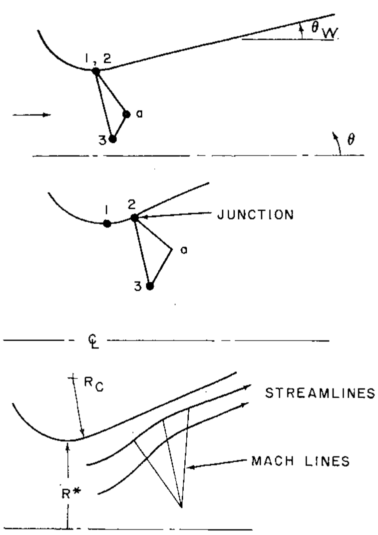

Fig. 1 Flow field and nomenclature.

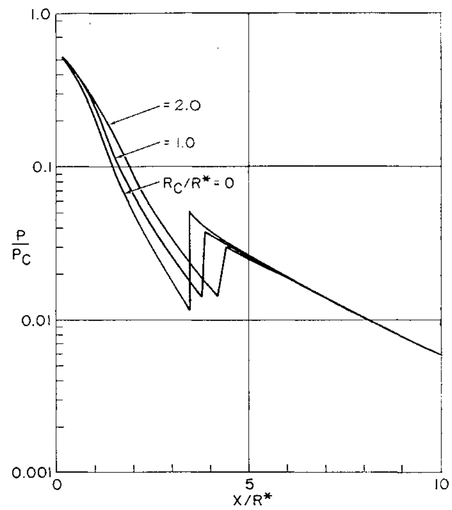

Fig. 2 Shock strength and location.

With the nomenclature of Figs. 1a and 1b, lines 2a and 3a represent right and left running characteristics, respectively, and the expansion from point 1 to point 2 occurs at the beginning of the conical section. Then the flow angle at point $a(\theta_a)$ is found to be greater than the inviscid flow angle at the wall ($\theta_2 = \theta_w$). This overturning of the flow can be shown analytically with the following assumptions: assume region 1-2 shrunk to a point as in Fig. 1a, point 3 sufficiently close to point 1 so that flow conditions at both points are identical and that the initial flow is parallel ($\theta_1 = \theta_3 = 0$). Then a Prandtl-Meyer turn from θ_1 to θ_2 produces the right running expansion line 2a. Using a standard characteristic solution for point a, the first-order difference scheme results in

$$\theta_a - \theta_2 = \frac{\left[\dfrac{\sin\theta_2 \sin\alpha_2 \tan\alpha_2}{\cos(\theta_2 - \alpha_2)} \dfrac{\epsilon(x_a - x_2)}{y_2}\right]}{[(W_1/W_2)\tan\alpha_1 + \tan\alpha_2]}$$

where W is velocity, α is the Mach angle, $\epsilon = 1$ for axisymmetric flow, and zero for planar flow. From the preceding results, it follows that $\theta_2 = \theta_a$ in planar flow (as it should be) but that $\theta_a > \theta_2$ for axisymmetric flow.

In the design of shock-free optimum shaped axisymmetric nozzles,[6,7] an initial region of the supersonic contour is arbitrarily specified, and the contour downstream of this region is determined. This downstream contour contains a slight increase in wall angle before turning the flow back toward the axial direction (to accommodate the overturning mentioned previously). This suggests that shock-free conical nozzles can be obtained by attaching the cone tangent to the optimum shaped contour at any point downstream of the maximum wall angle. Our studies as well as the results contained in Ref. 2 indicate that this method eliminates the formation of shocks.

References

[1] Migdal, D. and Landis, F., "Characteristics of conical supersonic nozzles," ARS J. **32,** 1898–1901 (1962).

[2] Darwell, H. M. and Bradham, H., "Shock formation in conical nozzles," AIAA J. **1,** 1932–1934 (1963).

[3] Lezberg, E. A. and Franciscus, L. C., "Effects of exhaust nozzle recombination on hypersonic ramjet performance: 1. Experimental measurements," AIAA J. 1, 2071–2076 (1963).

[4] Chen, C. J., "Experimental investigation of atomic recombination in a supersonic nozzle," J. Fluid Mech. 17, 450–458 (1963).

[5] Migdal, D., "Chemical nonequilibrium in nozzle flows," Grumman Aircraft Engineering Corp., Rept. ADR-01-10-64.1 (1964).

[6] Ahlberg, J. H., Hamilton, S. A., Migdal, D., and Nilson, E. N., "Truncated perfect nozzles in optimum nozzle design," ARS J. 3, 614–620 (1961).

[7] Rao, G. V. R., "Exhaust nozzle contour for optimum thrust," Jet Propulsion 28, 377–382 (1958).

Unsteady Flow Phenomena in Nozzles

BENJAMIN E. NEVIS*
Lehigh University, Bethlehem, Pa.

Nomenclature

a = speed of sound
A = nozzle cross-sectional area
L = nozzle length
M = Mach number
P = pressure
t = time
x = length
γ = ratio of specific heats
λ = $(x/A)(dA/dx)$

Subscripts

b = back or surrounding pressure
e = nozzle exit
0 = stagnation
$*$ = nozzle throat

SINCE the early 1950's, several investigations have been made of the unsteady or "start-up" flow phenomena in nozzles.[1–3] All of this work has been chiefly of an analytical nature with little quantitative experimental corroboration. To alleviate this situation, an analytical and experimental study of these phenomena was made at Lehigh University.[4]

The particular problem investigated involved a two-dimensional nozzle of hyperbolic contour attached to large reservoir initially containing a stagnant pressurized gas. Gas flow was initiated through the bursting of a membrane at the nozzle exit, the gas discharging directly into the surroundings. The nozzles are operated under the conditions shown in Table 1.

Excluding regions containing or affected by shock waves, the transient flow fields in the nozzles were considered to be the quasi-one dimensional, unsteady, adiabatic, homentropic flow of a compressible ideal gas ($\gamma = 1.4$). The continuity, momentum, and energy equations corresponding to these flow fields form a system of hyperbolic, quasi-linear, first-order partial differential equations. They were solved by the method of characteristics employing DeHaller's graphical-numerical technique.[5] The boundary conditions were: a) zero velocity and initial stagnation pressure at the nozzle inlet, b) pressure at the exit equal to that of the surroundings for subsonic outflow and determined by the characteristic net for supersonic outflow, c) flow-boundary contour was the physical-boundary contour, d) membrane burst generated a centered rarefaction wave. An example of the solutions is shown in Fig. 1 where the physical plane is sketched for the Mach 2.0 nozzle ($P_b/P_0 = 0.744$). From the physical and state planes, the theoretical pressure-time curves were determined at locations I, II, and III.

Table 1 Conditions for nozzle operation

Nozzle	$\frac{A_e}{A_*}$	$\frac{P_b}{P_0}$	Steady flow operating characteristics
Convergent	1.0	0.528	$M_e = 1.0$
Convergent-divergent	1.04676	0.38606	$M_e = 1.25$
Convergent-divergent	1.6875	≤ 0.278	$M_e = 2.0$
Convergent-divergent	1.6875	0.744	Stationary normal shock at $A/A_* = 1.3376$

Received March 23, 1965; revision received May 21, 1965. The author thanks his thesis advisor Jerzy A. Owczarek, for his encouragement and assistance during the course of this work.

* Assistant Professor, Department of Mechanical Engineering.

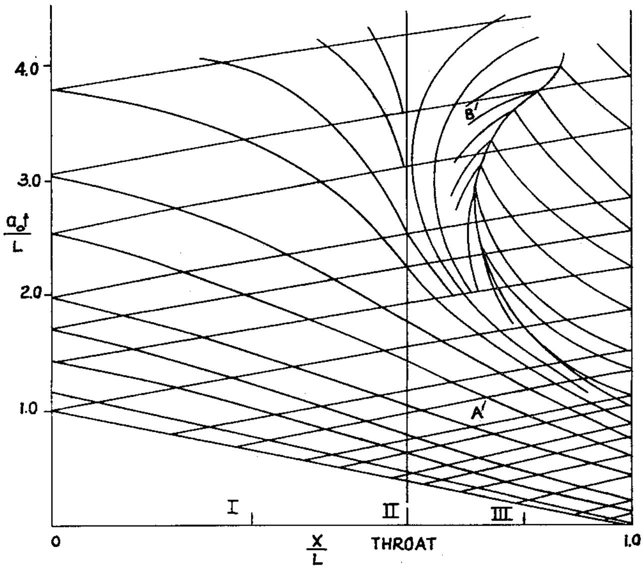

Fig. 1 Physical plane, Mach 2.0 nozzle ($P_b/P_0 = 0.744$).

The experimental variation of pressure vs time was measured by Kistler piezoelectric crystal pressure transducers (rise time 6–7 μsec, natural frequency $\simeq$ 80,000 cps) with readout on a Tektronix Type 555 dual beam oscilloscope. The gas used was dry nitrogen (dew point $-73°F$). The data were reproducible to within the thickness of the scope trace.

Typical theoretical and experimental dimensionless pressure-time curves with corresponding error ranges are shown in Fig. 2. With the exception of the case involving the shock wave (and only for the latter stages of the transient at station III) the major qualitative trends predicted by theory were followed by the experimental curves, although the latter were quantitatively higher and lagged behind the former. The disagreement between the curves at station III for the shock-wave case was probably due to shock-wave bifurcation. Steady flow experiments[6] revealed that shock waves of the strength encountered for this case bifurcate completely forming a "pseudo" shock wave, which extends throughout the rest of the divergent section. This results in a higher pressure than predicted at station III.

In order to determine the factors causing the quantitative discrepancies (too large to be due to experimental error), a re-evaluation was made of the initially postulated assumptions employed in the theory. This investigation revealed that discrepancies were due principally to the following incorrect assumptions:

1) Assumptions that the inital rarefaction wave was centered, the inlet boundary condition was zero velocity, and initial reservoir pressure was immediately adjacent to the inlet:

Previous investigators[7,8] have shown that the bursting of a membrane does not produce a centered rarefaction wave.